

# Potential of thermogravimetric analysis coupled with mass spectrometry for the evaluation of kerogen in source rocks

Craig P. Marshall<sup>a</sup>, G.S. Kamali Kannangara<sup>a</sup>, Michael A. Wilson<sup>a,\*</sup>,  
Jean-Pierre Guerbois<sup>a</sup>, Birgitta Hartung-Kagi<sup>b</sup>, Gwenda Hart<sup>b,†</sup>

<sup>a</sup>*Organic Geochemistry Group, Department of Chemistry, Materials and Forensic Science, University of Technology, Sydney, P.O. Box 123, Broadway, 2007, Australia*

<sup>b</sup>*Geotechnical Services Pty Ltd., Locked Bag 27, Cannington 6107, Australia*

Received 28 February 2001; accepted 1 August 2001

## Abstract

The molecular composition of oil and yield from a source rock depends on the temperature to which the source rock is subjected. However, the yield of oil and gas represents hydrocarbons generated over a range of temperatures. A technique that measures both volatile yields and bulk and molecular compositions during volatile evolution would determine the differential effects of temperature change, thereby giving information on the effect of thermal gradients. Attaching a mass spectrometer to a thermogravimetric analyser assists in this goal since it allows gases to be analysed during petroleum source rock evaluation by pyrolysis. Single ion monitoring allows unambiguous identification of thermal events. It reveals temperature at which water, methane and carbon dioxide evolve. This allows organic and inorganic transitions to be distinguished. Parameters that describe the yields of oil and gas can also be derived from thermogravimetric analysis (TGA) in much the same way as they can for Rock–Eval pyrolysis data and are useful when combined with solid state <sup>13</sup>C nuclear magnetic resonance (NMR) spectroscopy and Rock–Eval data for elucidating mineral matter effects. © 2002 Elsevier Science B.V. All rights reserved.

*Keywords:* Kerogen; Pyrolysis; Thermogravimetric analysis; Mass spectrometry; Source rocks; Petroleum

## 1. Introduction

The principal objective in petroleum source rock evaluation is to determine the petroleum generation potential of the sample and the petroleum generation relationship to neighbouring samples. Rock–Eval

pyrolysis is a method used to evaluate the oil and gas potential and the maturity of source rocks during petroleum exploration (Espitalie et al., 1977). The sample is heated, and the yield of material volatilised below 300 °C (termed S1) is a measure of the hydrocarbon present in the rock in a free or absorbed state. The yield of volatile material generated by thermal cracking at 300–500 °C (S2) measures the potential of the source rock to yield oil. In a more recent variant (Rock–Eval pyrolysis II) (Peters and Moldowan, 1993) the material evolved after this temperature (S3) is determined by oxidation. During

\* Corresponding author. Tel.: +61-2-9514-1761; fax: +61-2-9514-1628.

E-mail address: Mick.Wilson@uts.edu.au (M.A. Wilson).

† Deceased.

pyrolysis, the temperature  $T_{\max}$ , recorded at the maximum rate of volatile release is also measured and used to evaluate thermal maturity of the source rock.

Rock–Eval pyrolysis does not afford information on the composition of the source rock or the oil derived from it other than yields of volatile material at different temperatures. Oil quality is usually measured by gas chromatography mass spectrometry (GC/MS). However, GC/MS gives information only on materials that can pass through a GC column and be identified.

Solid state  $^{13}\text{C}$  nuclear magnetic resonance (NMR) spectroscopy can also be useful. It is possible to estimate the aromaticity of a petroleum prone source rock and the oil that is evolved from that rock at different temperatures (Maciel et al., 1978; Miknis et al., 1982a,b; Wilson et al., 1994) thereby providing additional information. Nevertheless solid state  $^{13}\text{C}$  NMR spectroscopy is insensitive and measurements on source rocks with carbon (<20%) involve overnight runs on individual samples. Solution NMR spectroscopy is useful but like GC/MS it only gives information about the product oil and not what is going on in the source rock.

A technique that measures both volatile yields and bulk and molecular compositions during volatile evolution would be ideal for source rock evaluation. Only progress towards this goal has been made, but thermogravimetric analysis (TGA) coupled with some mode of volatile matter detection appears to have promise. During TGA, the sample to be analysed is heated and its mass loss monitored. Ottaway (1982) used TGA to provide a measure of the volatile matter in coals and cokes. Huang et al. (1999) performed TGA of coals ranked from lignite to anthracite, and showed that the maximum temperature for volatile matter evolution correlated strongly with vitrinite reflectance. Espitalie et al. (1977) and Madec and Espitalie (1984) used TGA to detect total hydrocarbons in kerogens for petroleum source rock evaluation. In an interesting variant, Claypool and Reed (1976) used flame-ionization detection with TGA to detect only hydrocarbons in the volatiles. The integrated response was directly proportional to the concentration of extractable hydrocarbons and the organic carbon content of the samples studied.

Various other detectors have been used. Whelan and Huc (Whelan et al., 1980; Huc and Hunt, 1980;

Huc et al., 1981) trapped the evolved TGA products from pyrolysis and analysed them by GC. The information gained by this technique, although useful, gives only bulk composition of oils over temperature ranges, and does not determine composition at thermal temperature. It cannot be ascertained for example, whether rearrangements occur during cooling. Carangelo et al. (1987) analysed the evolving volatiles derived from TGA by Fourier Transform infrared spectroscopy (FTIR) for several samples of source rocks. By monitoring the aliphatic peak at  $2700\text{--}3000\text{ cm}^{-1}$  the evolution rate of aliphatics was determined at different temperatures. Recently, we showed the potential of Emission FTIR spectroscopy in thermal analysis of kerogens for measuring similar parameters (Marshall et al., 2001). The technique has greater scope than conventional FTIR spectroscopy since the heated kerogen can be monitored during volatile evolution rather than just the cooled volatiles. Emission FTIR spectroscopy provides chemical composition of the source rock at reaction temperature, although it does not give composition of the volatiles at its present state of development.

In this paper, results are presented from a TGA instrument which has been coupled to a mass spectrometer in order to evaluate the composition of evolved gases. Single ion monitoring by mass spectrometry reveals clear inflections where chemical events are observed. This paper also compares traditional source rock evaluation techniques such as Rock–Eval pyrolysis data (S1, S2, S1+S2 and  $T_{\max}$  values) and solid state  $^{13}\text{C}$  NMR spectroscopy with TGA of kerogen samples measured on the same instrument, and uses the additional information available from single ion monitoring to elucidate the role of the mineral matter present during pyrolysis.

## 2. Experimental

### 2.1. Samples

Sample locations are not reported due to commercial sensitivities. Elemental compositions are given in Table 1. Carbon, hydrogen and nitrogen elemental compositions were determined on a Carlo Erba 1106 instrument performed by the Microanalytical Unit, Research School of Chemistry, Australian National

University (ANU), Canberra, Australia. Samples were ground to fine powders before the study. % Carbon was determined by Rock–Eval analysis. Samples were air dried before analysis at room temperature under vacuum at ANU.

Mineral analyses of the source rock samples were obtained by X-ray diffraction spectroscopy. A Siemens Kristalloflex X-ray generator equipped with two powder cameras with Bragg–Brentano geometry was used. A Philips PW2276/20 X-ray tube was used at a power of 30 mA and 45 kV to produce cobalt X-rays. Samples were mounted in an aluminium sample holder. The holder and sample were balanced on the diffractometer and an XRD pattern collected from  $3.00^\circ$  to  $90.00^\circ 2\theta$ , at intervals of  $0.02^\circ 2\theta$ . Count times varied, but usually 4 s per interval was employed, to give a total count time of 4 h for the 2176 data points per scan. X-ray diffractograms are shown in Fig. 1.

Rock–Eval analyses have been reported elsewhere (Marshall et al., 2001) but are shown again in Table 2 for correlation purposes. Rock–Eval pyrolysis parameters are defined as: S1=volatile hydrocarbons (150–300 °C), S2=hydrocarbons generating potential (300–500 °C), S3=carbon dioxide produced by combustion of material not distilling below 500 °C, S1+S2=potential yield,  $T_{\max}$ =temperature of maximum oil yield during S2 oil generation, PI=production index =  $S1/(S1+S2)$ , TOC=total organic carbon (g/100g), HI=hydrogen index =  $(S2/TOC)100$  (mg/g) and OI=oxygen index =  $(S3/TOC)100$  (mg/g).

Table 1  
Elemental data for samples

Sample	%C	%H	%N	H/C mole ratio
1	0.51	0.088	0.053	2.07
2	1.14	0.23	0.00	2.42
3	2.22	0.65	0.089	3.51
4	4.00	0.45	0.090	1.35
5	7.21	0.92	0.23	1.53
6	14.76	2.39	0.49	1.94
7	23.70	2.25	0.27	1.14
8	32.20	2.83	0.67	1.06
9	40.50	3.31	0.91	0.98
10	52.76	3.24	0.77	0.74
11	64.30	4.28	1.35	0.80

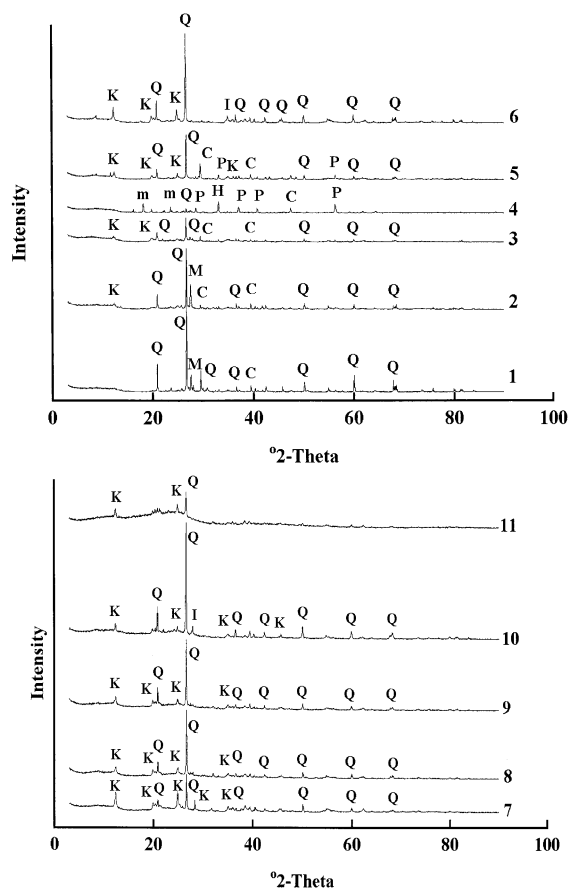


Fig. 1. X-ray diffraction patterns for samples 1 through to 11 from  $3^\circ$  to  $90^\circ$ . Q=Quartz, M=Microcline, K=Kaolinite, I=Illite, m=Montmorillonite, C=Calcite, H=Hematite and P=Pyrite. Numbers refer to sample numbers.

## 2.2. Solid state $^{13}\text{C}$ nuclear magnetic resonance (NMR) spectroscopy

Solid state  $^{13}\text{C}$  NMR spectra were obtained on a Bruker DRX 200-MHz instrument using cross-polarisation (CP) and magic angle spinning (MAS) of  $54.7^\circ$  to the applied field. The kerogens were packed into 4-mm zirconia rotors with Kel-F caps and spun at a speed between 7 and 10 kHz. The CP experiments required up to 150 000 transients with a contact time of 1 ms and recycle delay of 2s. Spectra were collected in 1 K points, zero filled to 4 K and then Fourier transformed using a line broadening factor of 50 Hz to

Table 2  
Source rock parameters determined from Rock–Eval pyrolysis and TGA/MS experiments

No.	S1 (mg/g)	TGA S1 (mg/g)	S2 (mg/g)	TGA S2 (mg/g)	S3 (mg CO <sub>2</sub> /g)	TGA S3 (mg CO <sub>2</sub> /g)	S1 + S2 (mg/g)	TGA S1 + S2 (mg/g)	$T_{\max}$ (°C)	TGA $T_{\max}$ (°C)	PI	TGA PI	TOC (%)	HI (mg/g TOC)	TGA HI (mg/g TOC)	OI (mg CO <sub>2</sub> /g TOC)	TGA OI (mg CO <sub>2</sub> /g TOC)
1	0.05	2.0	0.18	67.00	1.22	46.80	0.23	69.0	N/D	N/D	0.22	0.029	0.51	35	13137	239	9176
2	0.10	6.0	0.59	77.00	3.06	54.70	0.69	83.0	416	400	0.14	0.072	1.14	52	6754	268	4798
3	0.09	13.0	0.64	94.00	2.19	89.50	0.73	107.0	414	400	0.12	0.121	2.22	29	4234	99	4032
4	1.32	23.0	8.10	111.0	0.07	151.5	9.42	134.0	454	493	0.14	0.172	4.00	203	2775	2	3788
5	3.02	32.0	25.37	111.0	0.84	146.6	28.39	143.0	442	496	0.11	0.224	7.21	352	1540	12	2033
6	5.05	38.0	16.17	90.00	1.68	64.20	21.22	128.0	457	502	0.24	0.296	14.76	110	610	11	435
7	6.04	N/D	57.17	N/D	1.93	N/D	63.21	N/D	438	N/D	0.10	N/D	23.70	241	N/D	8	N/D
8	3.53	39.0	49.00	162.0	9.68	153.2	52.53	201.0	427	446	0.07	0.194	32.20	152	503	30	476
9	3.87	38.0	49.05	207.0	10.5	137.8	52.92	245.0	427	525	0.07	0.155	40.50	121	511	26	340
10	7.57	42.0	84.94	243.0	2.12	112.4	92.51	285.0	465	498	0.08	0.147	52.76	161	461	4	213
11	3.71	27.0	135.2	287.0	8.28	161.3	138.9	314.0	438	580	0.03	0.086	64.30	210	446	13	251

S1 = volatile hydrocarbons, TGA S1 = % mass loss between 150 and 300 °C × 10 (convert g/100 g to mg/g), S2 = hydrocarbon generating potential, TGA S2 = % mass loss between 300 and 500 °C × 10 (convert g/100 g to mg/g), S3 = organic carbon dioxide, TGA S3 = assume that total % mass loss is carbon from organic matter so, (% mass loss/12) × 44 × 10 (convert g/100 g carbon to mg/g CO<sub>2</sub>), S1 + S2 = potential yield,  $T_{\max}$  = the temperature of maximum weight loss by Rock–Eval for S2, TGA  $T_{\max}$  = the maxima of the derivative of the TG curve for TGA S2, PI = production index S1/(S1 + S2), TGA PI = TGA S1/(TGA S1 + TGA S2), TOC = total organic carbon, HI = hydrogen index = 100S2 (mg/g)/TOC (g/100 g), TGA HI = 100TGA S2(mg/g)/TOC (g/100 g), OI = oxygen index = 100CO<sub>2</sub> (mg/g)/TOC(g/100 g), TGA OI = 100CO<sub>2</sub> TGA S3 (mg/100 g)/TOC (g/100 g) and N/D = no data.

obtain the frequency domain spectra. The low field peak of adamantane was employed as a secondary reference but data are reported relative to tetramethylsilane. Blanks were run of rotors to ensure no artifacts in the spectra. The fraction of carbon which is aromatic ( $f_a$ ) was measured directly from the spectra by integrating the signals from 0 to 100 ppm (aliphatic) and 100 to 170 ppm (aromatic). This ratio is defined as the integrated signal area of aromatic carbon divided by the summation of the integrated signal area of aromatic and aliphatic carbon. Details of the fraction of carbon that is aromatic ( $f_a$ ), fraction of aliphatic carbon ( $1 - f_a$ ) and the percentage carbon type per sample are given in Table 3. They are not absolute because of relaxation considerations (Wilson, 1987). They are, however, useful for comparative purposes.

### 2.3. Thermogravimetric analysis/mass spectrometry (TGA/MS)

The TGA/MS instrument consists of a Setaram setsys 16/18 thermobalance, which is coupled to a Balzers Thermostat quadrupole mass spectrometer. Approximately 10–15 mg sample of each kerogen was placed in an alumina crucible and heated in the thermobalance at 5 °C/min heating rate from ambient temperature to 1000 °C. All of the TGA analyses were performed in an argon atmosphere under 40 ml/min flow rate. The volatile pyrolysis products from the sample in the TGA apparatus are trans-

ferred via a quartz capillary to a transfer line in a heated jacket at 150 °C to the mass spectrometer. The gases then enter the ionisation chamber where electron impact was performed with 70 eV electron energy.

Rock–Eval pyrolysis equivalent parameters (Espitalie and Bordenave, 1993) such as S1, S2, S1+S2 and  $T_{max}$  were determined by TGA/MS. The percentage mass loss was calculated from the weight loss curve and used to determine S1 and S2 between 150–300 and 300–500 °C, respectively. The derivative of the TG curve, that is, the DTG was taken, to determine TGA  $T_{max}$ , the temperature at the maxima rate of evolution curve. Gases were monitored as ions at mass/charge ratios ( $m/e$ ) 44 ( $CO_2^+$ ), 18 ( $H_2O^+$ ), and 15 ( $CH_3^+$ ). These ions define the presence of  $CO_2$ ,  $H_2O$  and  $CH_4$ , respectively.

## 3. Results and discussion

### 3.1. Source rocks

Elemental compositions are shown in Table 1. For low carbon samples (samples 1–4) the H/C ratios are meaningless because of the difficulty in measuring low hydrogen contents. However for other samples the H/C ratio varies between 0.74 and 1.94. Samples were chosen which reflect the range of Rock–Eval pyrolysis data that may be encountered in petroleum exploration. The total organic carbon content of these samples varied from 0.51% to 64.30 % by weight. Samples were chosen which had both high (sample 10, Table 2) and low (sample 1, Table 2) free oil contents (S1), and variable hydrocarbon generating potential (S2) (compare samples 1 and 11, Table 2). Likewise the production index  $PI = S1/(S1 + S2)$  of samples examined varies from 0.03 to 0.24 and the hydrogen index ( $S2 \text{ (mg/g)/TOC (g/100 g)} \times 100$ ) can be very high (sample 5, Table 2) or very low (sample 1, Table 2). Similarly the oxygen index,  $OI = (S3 \text{ (mg/g)/TOC (g/100 g)} \times 100)$  varies considerably.

Table 3 shows the solid state  $^{13}C$  NMR spectroscopic data. For brevity spectra are not plotted since numerous spectra have been reported elsewhere (Wilson, 1987, Wilson et al., 1991, 1994). The spectra show resonances at 100–150 ppm, centered at approxi-

Table 3

Estimates of aromatic carbon ( $f_a$ ), aliphatic ( $1 - f_a$ ), percentage aromatic carbon ( $\%Cf_a$ ) and percentage aliphatic carbon ( $\%C(1 - f_a)$ ) of source rock samples as measured by solid state  $^{13}C$  NMR spectroscopy and elemental analysis

Sample	$f_a$	$1 - f_a$	$\%Cf_a$	$\%C(1 - f_a)$
1	0.76	0.24	0.39	0.12
2	0.82	0.18	0.93	0.21
3	0.72	0.28	1.60	0.62
4	0.76	0.24	3.04	0.96
5	0.57	0.43	4.11	3.10
6	0.86	0.14	12.69	2.07
7	0.48	0.52	11.38	12.32
8	0.42	0.58	13.52	18.68
9	0.43	0.57	17.41	23.09
10	0.62	0.38	32.71	20.05
11	0.53	0.47	34.08	30.22

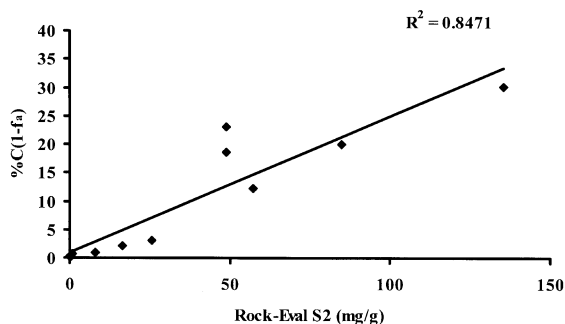


Fig. 2. Plot of  $\%C(1 - f_a)$  versus Rock-Eval pyrolysis S2. There are 11 points, some plot on the same coordinates.

mately 130 ppm, which is assigned to aromatic carbon (Wilson, 1987). In addition to the main aromatic carbon resonance, there is a slight shoulder at approximately 150 ppm, which is attributed to phenolic and aromatic ether carbons. Smaller resonances also, at 0–50 ppm, centered at approximately 30–40 ppm are assigned to alkyl carbons (methyl, methylene and methyne) and methylene in long alkyl chains and a few carbons removed from the end of the chain (Wilson, 1987). Some spectra show trace resonances at approximately 170 ppm that is attributable to the C=O carbon in carboxylate functionality.

Table 3 shows the fraction of aromatic carbon, that is,  $f_a$  present within each sample and also aliphatic carbon,  $1 - f_a$ . A number of workers have shown that for kerogens (Wilson, 1987; Maciel et al., 1978, 1979; Miknis, 1982; Miknis et al., 1979, 1982a,b; Miknis and Netzel, 1982), S2 yield correlates with  $(1 - f_a)$ . Free (S1) oil would not be observed by solid state  $^{13}\text{C}$  NMR spectroscopy, hence only S2 and S3 yielding carbon should be seen directly by  $^{13}\text{C}$  NMR spectroscopy. For the correlation to hold this means that during pyrolysis, any oil which is derived from aromatic carbon must balance almost exactly any aliphatic carbon which is fixed by coking reactions and is involatile. Such transformations are likely to be mineral matter dependent since clays and other aluminosilicates can act as cracking catalysts in source rocks (Espitalie et al., 1984; Huizinga et al., 1987; Wilson et al., 1986). There could however be a correlation for source rocks if the dilution effects of mineral matter are taken into account, that is S2 is plotted against  $\%C(1 - f_a)$ . This will only hold if the minerals present

are not catalysing cracking or coking reactions. It is well known that clay minerals such as montmorillonite, illite and kaolinite (Espitalie et al., 1984; Huizinga et al., 1987), and other aluminosilicates for example, microcline (Wilson et al., 1986) can crack oil and affect yields. Fig. 2 shows that for the samples studied here there is a good correlation of S2 with  $\%C(1 - f_a)$  if samples 8 and 9 were left out. With these included the correlation is only moderate ( $R^2 = 0.8471$ ). It is significant that the source rocks with highest  $1 - f_a$  (around 0.6) values are off the line. These source rocks also contain kaolinite. Sample 4 also contains haematite and pyrite which can catalyse rearrangements and cause in situ hydrogenation (Mukherjee and Chowdhury, 1976; Whitehurst et al., 1980; Burnham and Happe, 1984; Smeulders et al., in press). These results show quite clearly that haematite and pyrite are unimportant in these systems but when there are large amounts of aliphatic chains mineral matter can play some role. Mineral matter effects are not the overriding factor because if they were, there would be no correlation with  $\%C(1 - f_a)$ .

### 3.2. Thermogravimetric mass spectrometric analysis (TGA/MS)

Fig. 3 shows the derivative mass loss curves (DTG thermograms) during the pyrolysis of the

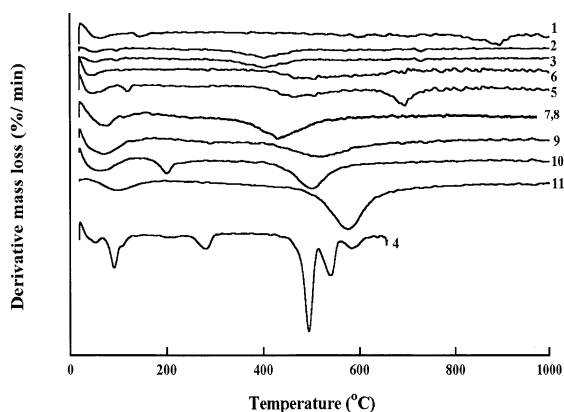


Fig. 3. DTG Thermograms of selected samples. The y-axis is the differential ( $\partial\text{mass}/\partial\text{time}$ ) and is (g/100 g)/min. The samples have been stacked for easy visual inspection and hence the scale is not shown since it is displaced for each sample.

kerogen samples, respectively. The  $y$ -axis is the differential ( $\partial\text{mass}/\partial\text{time}$ ) and is (g/100 g)/min. The samples have been stacked for easy visual inspection and hence the scale is not shown since it is displaced for each sample. These thermograms reflect both the amount and type of organic matter present and the mineral matter content. Thus sample 1 shows little mass loss because it is largely quartz and contains only 0.51% carbon. Sample 11 on the other hand contains 64.30% carbon and hence gives a large mass loss centred at 580 °C. These thermograms also reflect the different volatility of the organic matter. In sample 8, most organic matter is volatile around 446 °C while for sample 10 this is closer to 500 °C. Sample 4 has been displaced to the bottom of the traces for clarity since it is unique in that multiple events can be observed. It has quite different mineralogy (Fig. 1).

The TGA data can be used to calculate Rock–Eval pyrolysis like data concerned with mass loss rather than yields of volatiles. The percentage mass loss was calculated from the TG curve and used to determine S1 and S2 between 150–300 °C and 300–500 °C, respectively. These are given in Table 2 with conventional Rock–Eval pyrolysis data and are expressed in the same way. The difference between the TGA values and the Rock–Eval pyrolysis values is an indication of gas yields. These can be calculated by the differences in Table 2. They include of course, water and carbon dioxide.

A weak correlation was found between Rock–Eval pyrolysis S1 and TGA S1 ( $R^2=0.7932$ ). This illustrates that variable amounts of water are present in the samples and carbon dioxide forming structures. A reasonable correlation ( $R^2=0.9274$ ) was expressed by plotting Rock–Eval pyrolysis S2 against TGA S2 and there is a reasonable correlation between the percentage carbon in the rock which is aliphatic,  $\%C(1-f_a)$  and TGA S2 ( $R^2=0.9192$ , Fig. 4). This shows that most of the gas as well as the liquids originate from aliphatic carbon. It is noteworthy that samples 8 and 9 with high aliphatic contents and apparent effects of mineral matter now correlate better than with Rock–Eval S2. This is strong evidence that it is cracking reactions that cause samples 8 and 9 to deviate in Fig. 2.

$T_{\text{max}}$  values do not correlate well since gas forming cracking reactions may occur at slightly higher temper-

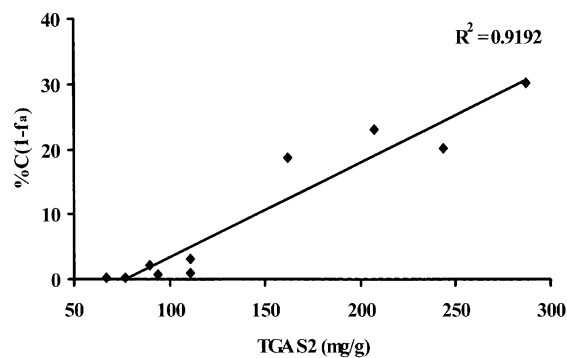


Fig. 4. Plot of  $\%C(1-f_a)$  versus TGA S2.

atures and are observed by TGA and not Rock–Eval pyrolysis. It is notable that normally values are higher for TGA  $T_{\text{max}}$  as opposed to Rock–Eval pyrolysis  $T_{\text{max}}$  values. The difference is particularly high for sample 9, which means there must be a greater ratio of gas relative to liquids evolved for this sample compared with other samples.

The hydrogen, production and oxygen indexes can also be calculated for TGA data (Table 2) but the terms tell us nothing about geochemical prospectivity. The low carbon content samples (7.2% C and less) have very high TGA hydrogen and TGA oxygen indexes because of the large amount of water vapour and gas that is evolved from inorganic components. With the exception of the samples 1–3 that contain very little oil, the TGA production indexes are much larger than their Rock–Eval counterparts because water is included and is shown in S1 at lower temperatures.

### 3.3. Single ion monitoring

Single ion monitoring allows the inflections in the DTG thermograms to be identified. Selected traces are shown in Fig. 5 to illustrate the point. Traces were obtained on all samples, and results are similar but in some yields are low and in others there was influence from base line drift. In effect, detector response is dependent on mass, and there should be a general relationship between yield of volatiles and detector response, but in the work reported here, the results have not been calibrated.

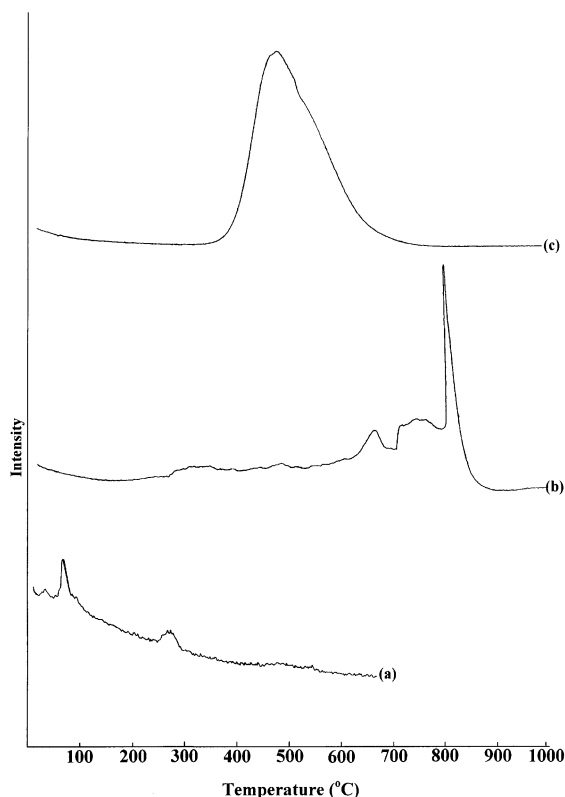


Fig. 5. Single ion monitoring thermal plot for (a)  $m/e$  18 ( $H_2O$ ) sample 4, (b)  $m/e$  44 ( $CO_2$ ) sample 3 and (c)  $m/e$  15 ( $CH_4$ ) sample 10. The  $y$ -axis is proportional to moles, but has not been calibrated.

Not surprisingly, small loss of mass is experienced at or below 100 °C from water and signals are observed for  $m/e$  18 at around 100 °C (an example is given in Fig. 5). There is also a steady stream of water loss before and after 400 °C, the latter because of water formed during thermal loss of organic oxygen as water and through some mineral dehydroxylation. Sample 4 contains haematite and pyrite (Fig. 1) which are potential organic matter decomposition catalysts and the transition around 280 °C is therefore difficult to assign. It is not clear from TGA alone whether this could be from catalytic thermal decomposition of organic matter by the haematite or pyrite to yield carbon dioxide or methane. These gases are absent in the  $m/e$  44 and 15 single ion monitoring traces for these substances. However, Fig. 5 (trace a) shows this is due to water. Probably

these minerals contain some tightly bound water that is released at this temperature. Single ion monitoring can confirm other dehydroxylation such as in kaolinite and illite (Corino and Turnbull, 1984) but the presence of the mineral was not sufficient to observe them here.

Fig. 5 (trace b) shows a  $m/e$  44 plot for sample 3 that contains calcite. Pure calcite decomposes normally at 889 °C (Barin et al., 1977) but the results clearly show that this decomposes in these samples at about 820 °C. There is a DTG inflection here (Fig. 3) but it is small and hard to see unless the figure is expanded. Variations in the temperature of decomposition were observed for other samples containing calcite.

Shown in Fig. 5 (trace c) is the typical evolution of methane. Methane evolution appears for all samples at 400 °C although in the samples with low carbon contents it is detected in low amounts. For samples 4 and 5 which are the only samples containing pyrite (Fig. 1), a second inflection was observed approximately at 630 °C. This inflection is seen in the DTG thermogram (Fig. 3). The inflection is clearly identified as being an organic transition and that pyrite is probably the catalytic agent. This information is not available using TGA alone. These results illustrate that TGA/MS is a valuable tool for investigating discrete differences between source rock samples.

The TGA/MS data single ion monitored for a specific product should not necessarily follow the simple TGA differential mass curves because a range, of products rather than one are evolved and recorded in a simple TGA experiment. However for methane and water there are clear correlations. For example, the sharp peak at 100 °C in Fig. 5 (trace a) matches the same peak in Fig. 3 for sample 4. The broad methane peak evolutions, Fig. 5 (trace c), follow the broad peaks in Fig. 3. A trace from sample 10 is shown which begins evolution at 400 °C, maximises at 469 °C in both samples and tails to 650 °C. In fact, both plots show the same tailing. The carbon dioxide curves are somewhat different in that the mass spectrometer appears very sensitive. This probably reflects that a little mass loss from carbonate minerals produces a relatively large amount of carbon dioxide. For methane, other mass loss products such as oil are lost at the same time, and for water the method is



insensitive because of constant bleed of water from the sample. Later work on quantitation will follow.

Single ion monitoring could also be carried out on higher molecular weight ions to detect the evolution of small organic molecules. However since there is no compound resolution it is not clear where they originate. Ions at  $m/e$  77 ( $C_6H_5$ ) and 91 ( $C_7H_7$ ) could be useful.

How does this help the exploration geologist? Ideally, one measurement by Rock–Eval pyrolysis and TGA/MS could provide a powerful matrix of complementary information to the petroleum exploration geologist. Rock–Eval pyrolysis gives no information on methane yields, which are a useful product, or other gas yields. TGA/MS can ascertain if a source rock is primarily gas prone and thermogravimetric analysis coupled with mass spectrometry gives additional in situ sample reaction information, that is, chemical changes as the sample is reacting. Further work is needed on quantitation and with a little extra development oil yields could be measured at the same time. This would make Rock–Eval pyrolysis redundant.

#### 4. Conclusions

(1) TGA/MS has shown to be a valuable method for obtaining Rock–Eval like pyrolysis equivalent information during the pyrolysis of source rocks to evaluate their hydrocarbon generation potential. Newly derived TGA pyrolysis parameters, such as, (TGA S1), (TGA S2) can be used with Rock–Eval pyrolysis data to estimate gas yields by difference. Parameters that describe the yields of oil and gas can be derived from TGA in much the same way as they can for Rock–Eval pyrolysis data. TGA S2 versus  $\%C(1 - f_a)$  plots when combined with Rock–Eval plots are useful for establishing the catalytic effects of mineral matter. Good correlations exist for TGA S2 versus  $\%C(1 - f_a)$  plots as gas and liquids that originate from the same cracking process for these samples are both observed by TGA. When minerals affect gas and oil yields, the effect can be observed by deviations in the Rock–Eval S2 versus  $\%C(1 - f_a)$  plot but not the TGA S2 versus  $\%C(1 - f_a)$  plot.

(2) Combining mineralogy and Rock–Eval pyrolysis with solid state  $^{13}C$  NMR spectroscopy reveals

new information. There is a reasonable correlation of aromaticity with yield of volatiles. For many but not all these samples, montmorillonite, illite, kaolinite, haematite and pyrite do not affect oil yields.

(3) Mass spectrometry can be used to measure specific gas components during thermal analysis. Single ion monitoring reveals clear inflections where water, methane and carbon dioxide evolve. For water, initial loss of chemically bound water can be observed and during events beginning at 400 °C where covalent bond cleavage occurs. For methane, generation begins as late as 400 °C but appears to be completed by 700 °C. The profiles for carbon dioxide are much more complex with multiple events and some due to mineral decomposition as late as 810 °C.

#### Acknowledgements

We thank Dr. Rick Wuhrer and Ms. Katie McBean, University of Technology, Sydney, for assistance in X-ray diffraction measurements. EO

#### References

- Barin, I., Knacke, O., Kubaschewski, O., 1977. Thermodynamic Properties of Inorganic Substances. Springer-Verlag, New York.
- Burnham, A.K., Happe, J.A., 1984. On the mechanism of kerogen pyrolysis. *Fuel* 63, 1353–1356.
- Carangelo, R.M., Solomon, P.R., Gerson, D.J., 1987. Application of TG-FT-i.r. to study hydrocarbon structure and kinetics. *Fuel* 66, 960–967.
- Claypool, G.E., Reed, P.R., 1976. Thermal analysis technique for source rock evaluation: quantitative estimate of organic richness and effects of lithologic variation. *American Association of Petroleum Geologists Bulletin* 60, 608–626.
- Corino, G.L., Turnbull, A.G., 1984. Calorimetric studies of oil shales and shale products. *Proc. Second Australian Workshop on Oil shale, St. Lucia, Australia, December 6 and 7*, pp. 97–102.
- Espitalie, J., Bordenave, M.L., 1993. Source rock parameters. In: Bordenave, M.L. (Ed.), *Applied Petroleum Geochemistry*, Chap. II, vol. 2. Technip, Paris.
- Espitalie, J., Laporte, J.L., Madec, M., Marquis, F., Leplat, P., Paulet, J., Boutefeu, A., 1977. Methode rapide de caracterisation des roches meres de leur potentiel petrolier et de leur degre d'evolution. *Revue de l'Institute Francais du Petrole*. 32, 23–42.
- Espitalie, J., Senga Makadi, K., Trichet, J., 1984. Role of the mineral matrix during kerogen pyrolysis. *Organic Geochemistry* 6, 365–382.
- Huang, H., Wang, S., Wang, K., Klein, M.T., Calkins, W.H., 1999. Thermogravimetric and Rock–Eval studies of coal properties and coal rank. *Energy and Fuels* 13, 396–400.

- Huc, A.Y., Hunt, J.M., 1980. Generation and migration of hydrocarbons in offshore South Texas Gulf coast sediments. *Geochimica et Cosmochimica Acta* 44, 1081–1089.
- Huc, A.Y., Hunt, J.M., Whelan, J.K., 1981. The organic matter of a Gulf coast well studied by a thermal analysis–gas chromatography technique. *Journal of Geochemical Exploration* 15, 671–681.
- Huizinga, B.J., Tannenbaum, E., Kaplan, I.R., 1987. The role of minerals in the thermal alteration of organic matter: III. Generation of bitumen in laboratory experiments. *Organic Geochemistry* 11, 591–604.
- Maciel, G.E., Bartuska, V.J., Miknis, F.P., 1978. Correlation between oil yields of oil shales and  $^{13}\text{C}$  nuclear magnetic resonance spectra. *Fuel* 57, 505–506.
- Maciel, G.E., Bartuska, V.J., Miknis, F.P., 1979. Improvement in correlation between oil yields of oil shales and  $^{13}\text{C}$  NMR spectra. *Fuel* 58, 155–156.
- Madec, M., Espitalie, J., 1984. Application of pyrolysis to the characterisation and the upgrading of the Toarcian oil shales from the Paris basin. *Fuel* 63, 1720–1725.
- Marshall, C.P., Wilson, M.A., Hartung-Kagi, B., Hart, G., 2001. Potential of emission Fourier transform infrared spectroscopy for in situ evaluation of kerogen in source rocks during pyrolysis. *Chemical Geology* 175, 623–633, NOTE: the units of TOC = total organic carbon are (g/100 g), and are given incorrectly in our previous paper.
- Miknis, F.P., 1982. NMR studies of solid fossil fuels. *Magnetic Resonance Review* 7, 87–121.
- Miknis, F.P., Netzel, D.A., 1982.  $^{13}\text{C}$  NMR measurements of the genetic potentials of oil shales. *Fuel* 46, 977–984.
- Miknis, F.P., Maciel, G.E., Bartuska, V.J., 1979. Cross polarization magic angle spinning  $^{13}\text{C}$  NMR spectra of oil shales. *Organic Geochemistry* 1, 169–176.
- Miknis, F.P., Smith, J.W., Maughan, E.K., Maciel, G.E., 1982a. Nuclear magnetic resonance: a technique for direct nondestructive evaluation of source-rock potential. *American Association of Petroleum Geologists Bulletin* 66, 1396–1401.
- Miknis, F.P., Szeverenyi, N.M., Maciel, G.E., 1982b. Characterisation of the residual carbon in retorted oil shale by solid state  $^{13}\text{C}$  NMR. *Fuel* 61, 341–345.
- Mukherjee, D.K., Chowdhury, P.B., 1976. Catalytic effect of mineral matter constituents in a North Assam coal on hydrogenation. *Fuel* 55, 4–8.
- Ottaway, M., 1982. Use of thermogravimetry for proximate analysis of coals and cokes. *Fuel* 61, 713–716.
- Peters, K.E., Moldowan, J.M., 1993. *The Biomarker Guide*. Prentice Hall, NJ.
- Smeulders, D.E., Wilson, M.A., Armstrong, L., 2001. Insoluble organic compounds in the Bayer process. *Industrial and Engineering Chemistry* (in press).
- Whelan, J.K., Hunt, J.M., Huc, A.Y., 1980. Applications of thermal distillation pyrolysis to petroleum source rock studies and marine pollution. *Journal of Analytical and Applied Pyrolysis* 2, 79–96.
- Whitehurst, D.D., Mitchell, T.O., Farcasiu, M., 1980. *Coal Liquefaction: The Chemistry and Technology of Thermal Processes*. Academic Press, New York.
- Wilson, M.A., 1987. *NMR Techniques and Applications in Geochemistry and Soil Chemistry*. Pergamon, UK.
- Wilson, M.A., McCarthy, S.A., Collin, P.J., Lambert, D.E., 1986. Alkene transformations catalysed by mineral matter in shale. *Organic Geochemistry* 9, 245–253.
- Wilson, M.A., Vassallo, A.M., Gizachew, D., Lafargue, E., 1991. A high resolution solid state nuclear magnetic resonance study of some coaly source rocks from the Brent Group (North Sea). *Organic Geochemistry* 17, 107–111.
- Wilson, M.A., Lafargue, E., Gizachew, D., 1994. Solid state  $^{13}\text{C}$  NMR for characterising source rocks. *Australian Petroleum Exploration Association Journal*, 210–215.